On the Interpretation of Ocean Current Spectra. Part 1: The Kinematics of Three-Dimensional Vector Time Series

JACK CALMAN[1]

Department of Earth and Planetary Sciences, Massachusetts Institute of Technology, Cambridge 02138

(Manuscript received 25 July 1977, in final form 27 February 1978)

ABSTRACT

A general method for representing and interpreting the spectra of three-dimensional vector time series is outlined. Part I contains the formalism for the kinematic interpretation of a single vector time series. Based on the spectrum density matrix, the formalism unifies and extends to three dimensions several descriptions of a vector process. These are the Cartesian, rotary, rotational invariant and hodograph spectrum representations. Empirical modes, which are properties of the measured time series (not of any geometrical or dynamical assumptions) are introduced. These allow independent orthogonal motions at the same frequency to be separated. Finally the notion of a prespecified spectrum, which automatically picks out that part of the measurement which is consistent with all imposed dynamical assumptions, is advanced.

1. Introduction

As oceanic and atmospheric measurements become more elaborate and expensive, it becomes important to develop and apply methods of analysis which can extract maximum information from the data. Similarly, as theories attempt to explain more details of the motion of the atmosphere and ocean, it becomes more important to make rigorous comparisons between theory and observations. Because physical phenomena vary as a function of frequency, measurements are usually described in the frequency domain where different theories apply in different frequency ranges. However, the fact that the velocity of the fluid is a vector is usually given minimal attention; the discussion is often confined to the rectangular components of the vector and their coherences with each other. The methods to be described exploit the fact that the velocity is a vector in the frequency domain (as opposed to progressive vector, stick diagrams and scatter plots, which are all in the time domain). This treatment gives much insight into the answers to the two fundamental questions—how is the fluid moving around? and why is it moving that way?

The standard decomposition of a vector into its Cartesian components and corresponding spectra can suffer from sensitivity to errors in the coordinate system orientation and from difficulty in deducing the kinematics of the motion for anything much more complicated than rectilinear motion. Because of these drawbacks, spectrum descriptions which do not depend on the orientation of the coordinate system, and which simply represent motions other than rectilinear oscillations have been developed.

One vector spectrum technique which has proven useful (see, e.g., Gonella 1972; and Mooers, 1973) treats the motion as being due to counterrotating waves. Current ellipses also give good insight into the nature of the motion (see, e.g., Thompson and Luyten, 1976). Certain spectrum quantities which are independent of coordinate system, the spectrum invariants, have also proven useful (Fofonoff, 1969).

In Part 1 a unified generalized Fourier representation of the vector spectra is developed in which each of the examples mentioned above appears as a particular case. All the representations are extended to three dimensions. A new representation for vector spectra is also introduced. At each frequency three empirical modes (for three dimensions) can be found which represent motions occurring simultaneously but independently. By means of these modes different physical processes may become distinguishable.

In Part 2, three different dynamical examples are chosen to illustrate some ways in which the various spectrum representations may be used to make tests of whether a set of measurements and a proposed theory are consistent. The three examples are wind forced surface currents (Pollard and Millard, 1970), internal waves (Fofonoff, 1969), and bottom-trapped topographic Rossby waves (Thompson, and Luyten, 1976).

[1] Present affiliation: Environmental Research and Technology, Inc., Concord, MA 01742.

0022-3670/78/0627-0643$08.50

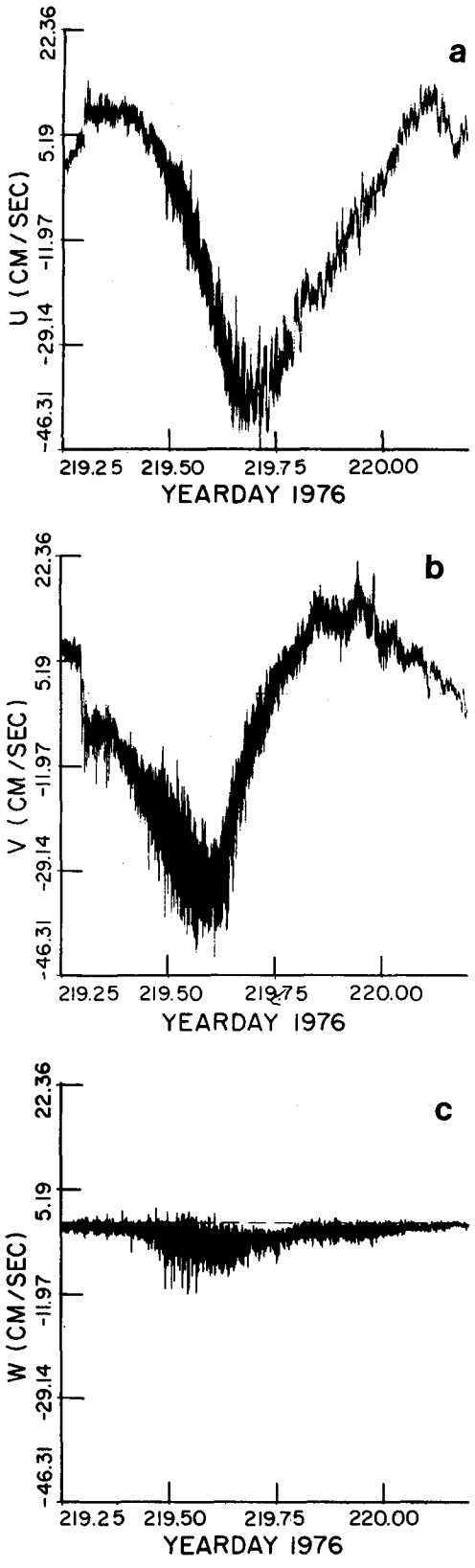

FIG. 1. Cartesian components of a typical three-dimensional vector time series measurement.

A discussion of the distribution theory for the various spectrum parameters is included, so that the problem of confidence limits can be approached. The paper concludes with some speculation about further developments and uses of these spectrum techniques.

2. Fundamentals

a. The Cartesian spectrum density matrix

In this section the basic definitions and notations for the standard Cartesian spectral representation of a vector time series are established. Suppose the typical quantity of interest is an ocean current—a three-dimensional vector which varies continuously for all time. The instrument will measure (with modifications due to its own sensitivity, response time, etc.) a sequence of numbers describing the magnitude and direction of the current vector at (usually) equally spaced intervals of time. If the three-dimensional vector is specified by a magnitude $V(t)$ and two directions $\theta(t)$ and $\phi(t)$, where $-\infty < t < \infty$, the measurement consists of the set of N numbers

$$\{V_n,\theta_n,\phi_n\} \quad n = 1, 2, 3, \ldots N,$$

where $V_n \equiv V(n\Delta t)$, $\theta_n \equiv \theta(n\Delta t)$, $\phi_n \equiv \phi(n\Delta t)$, and Δt is the time sampling interval. Following the usual procedure, these three numbers are immediately transformed into components of the velocity vector (u,v,w) along the three mutually orthogonal axes (x,y,z). (Hence the name Cartesian representation.) The measurement of the velocity vector is now given by three discrete time series and two parameters

$$\{u_n,v_n,w_n\},\ N,\ \Delta t$$

which are shown for a typical measurement in Fig. 1. (For the purposes of this paper it does not matter whether the vertical velocity component is measured directly or derived from temperature measurements.) The data shown in Fig. 1 were acquired in 85 m of water, 5 m above the bottom of New England's continental shelf, during the passage of a hurricane.

The distribution of power with frequency is most directly (though, as will be seen, not necessarily most simply or effectively) described by the power spectra of the three vector components. These spectra are derived from the Fourier series representation of the time series, which can be written as

$$\mathbf{V}(t) = \mathrm{Re} \sum_{m=1}^{N/2-1} \hat{\mathbf{V}}_m e^{if_m t}, \tag{1a}$$

where

$$\mathbf{V}(t) \equiv \begin{pmatrix} u(t) \\ v(t) \\ w(t) \end{pmatrix}, \tag{1b}$$

$$\hat{\mathbf{V}}_m \equiv \begin{pmatrix} \hat{u}_m \\ \hat{v}_m \\ \hat{w}_m \end{pmatrix} \equiv \begin{pmatrix} \hat{u}_1 \\ \hat{u}_2 \\ \hat{u}_3 \end{pmatrix} \equiv \begin{pmatrix} u_1 e^{i\theta_1} \\ u_2 e^{i\theta_2} \\ u_3 e^{i\theta_3} \end{pmatrix}, \quad (1c)$$

$f_m \equiv 2\pi m/N\Delta t$ and $\hat{\mathbf{V}}_m$ denotes the complex Fourier coefficient at frequency f_m. The actual Fourier coefficients are given by

$$\hat{\mathbf{V}}_m = [2/(N\Delta t)] \sum \Delta t \mathbf{V}_k(t) \exp(-i2\pi mk/N\Delta t)$$

but the computation of these coefficients is only of minor interest here. The Fourier coefficients will therefore be assumed known. The power spectra of the vector time series are given by the elements of the Cartesian spectrum density matrix which is *defined* by

$$S_{ij} \equiv \langle \hat{u}_i^* \hat{u}_j \rangle \quad (2)$$

where the asterisk denotes complex conjugate and the angle braces denote ensemble average. (In practice the ensemble average is often estimated by a frequency band average, which equivalence is allowed by the ergodic hypothesis.) *The subscript* m *has been dropped, it being understood that all spectrum quantities are functions of frequency.* The off-diagonal elements of S_{ij} are complex whose real and imaginary parts are more conveniently interpreted separately:

$$S_{ij} \equiv C_{ij} - iQ_{ij}, \quad (3)$$

where C_{ij} and Q_{ij} are the co- and quadrature-spectra, respectively. The normalized form of the off-diagonal elements of the SDM (spectrum density matrix) is the most common and convenient description of the relation between components. These are the complex coherences

$$\gamma_{ij} \equiv \frac{S_{ij}}{[S_{ii}S_{jj}]^{1/2}}. \quad (4)$$

The amplitude and phase of γ_{ij} is often used in dynamical hypotheses testing, examples of which will be given in Part 2. So far, the SDM **S** has been described for a single 3-D vector. **S** is then a 3×3 Hermitian matrix, with three real and three complex independent elements. The three-dimensional Cartesian SDM for the data of Fig. 1 is shown in Fig. 2. Since the SDM is Hermitian the off-diagonal elements in the lower left of the matrix are complex conjugates of those in the upper right and therefore need not be shown. Generalizations to more than one vector are easily made. For Fourier component vectors from two different measurements,

$$\hat{\mathbf{u}}^{(k)} = \begin{pmatrix} \hat{u}_1^{(k)} \\ \hat{u}_2^{(k)} \\ \hat{u}_3^{(k)} \end{pmatrix}, \quad k = 1, 2, \quad (5)$$

the cross-spectral density matrix (CSDM) is defined by

$$S_{ij}^{(kl)} = \langle \hat{u}_i^{(k)} \hat{u}_j^{(l)} \rangle \quad . \quad (6)$$

In three dimensions it is now a 6×6 Hermitian matrix. The information contained in the 2-vector, three-dimensional CSDM is pictured schematically in Fig. 3. An example of the use of this approach (in a spectrum representation yet to be described) is given in Part 2.

b. Simple motions in the Cartesian representation

1) RECTILINEAR MOTION

Suppose, at some particular frequency, the motion is oscillatory along some arbitrary line (perhaps determined by local topography) whose direction is given by $\mathbf{r} = \alpha\mathbf{i} + \beta\mathbf{j} + \gamma\mathbf{k}$. The Fourier component velocity vector is $\hat{u} = \alpha a_0$, $\hat{v} = \beta a_0$, $\hat{w} = \gamma a_0$, and $\theta_1 = \theta_2 = \theta_3$. The SDM is then

$$\mathbf{S} = \langle a_0^2 \rangle \begin{pmatrix} \alpha^2 & \alpha\beta & \alpha\gamma \\ & \beta^2 & \beta\gamma \\ & & \gamma^2 \end{pmatrix}. \quad (7)$$

If a measured SDM is real, the motion is rectilinear and the direction of **r** may be deduced. In particular, if the motion is rectilinear along one of the coordinate axes, say the x-axis, then $\alpha = 1$ and $\beta = \gamma = 0$, so that **S** contains only one nonzero element S_{11}. In this case the physical interpretation is easy. Different spectrum representations allow similar simplifications for different types of motions.

2) ELLIPTIC MOTION

Suppose the motion is elliptical in a vertical plane (as is the case, for example, for surface waves), which for simplicity may be taken as the y–z plane. Then

$$\hat{u} = 0, \quad \hat{v} = \alpha a_0 e^{i\theta}, \quad \hat{w} = \beta a_0 e^{i(\theta \pm \pi/2)}$$

(The $\pm$ in the phase of w is for rotation in either direction). The SDM is

$$\mathbf{S} = \langle a_0^2 \rangle \begin{pmatrix} 0 & 0 & 0 \\ & \alpha^2 & \pm i\alpha\beta \\ & & \beta^2 \end{pmatrix}. \quad (8)$$

If $\alpha = \beta$, the motion is circular. The signature for this type of motion is seen to be a pure imaginary off-diagonal element. Note that even for the simple case of elliptic motion, three nonzero elements are present. It will be shown below that a more appropriate representation can reduce the number of nonzero elements to unity in this case also. In general, as shown in Fig. 2, all the elements are nonzero, making the Cartesian spectrum representation not one of the simplest to interpret. Another drawback of the Cartesian representation is the fact that the elements S_{ij} change when the coordinate

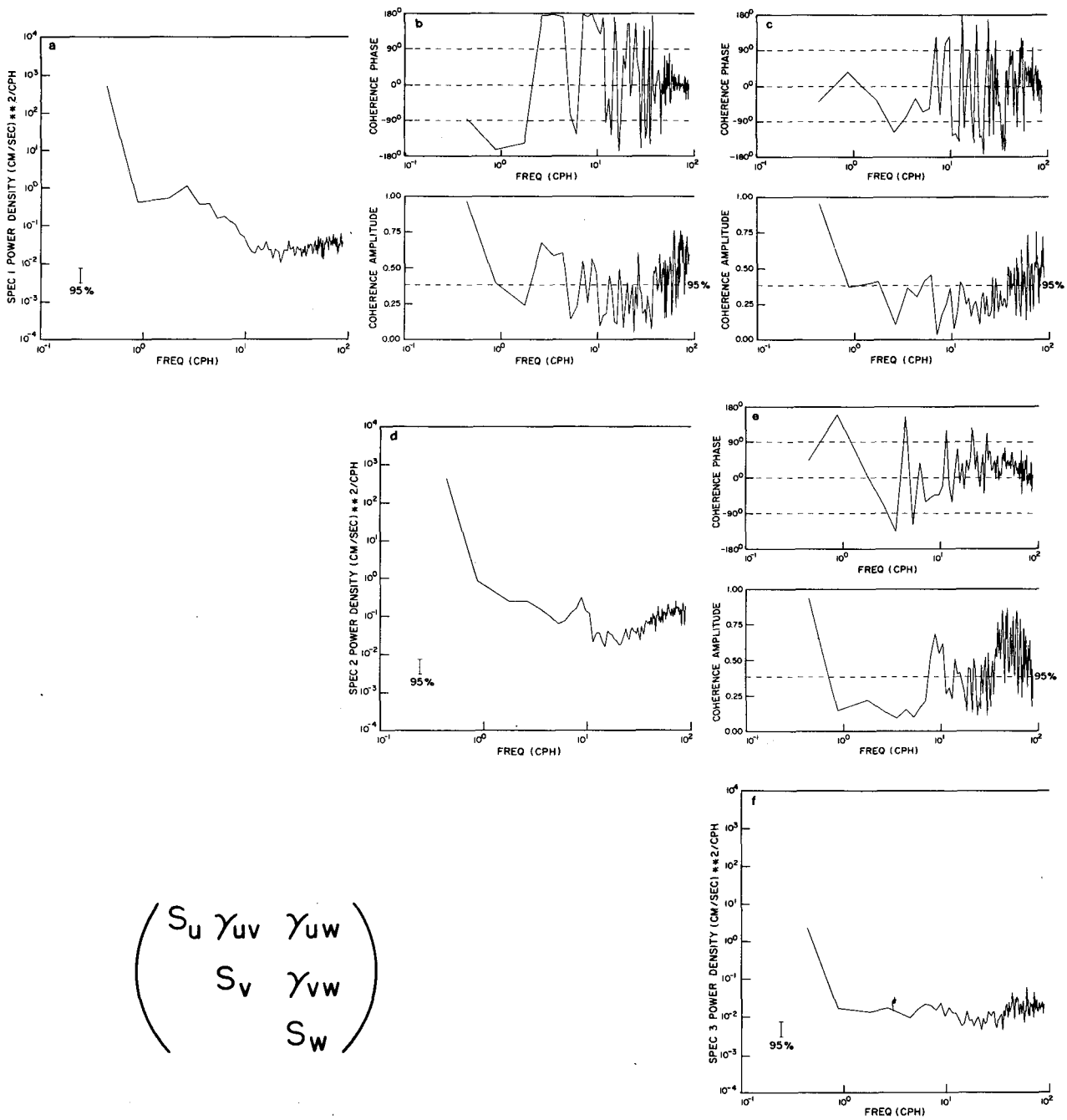

$$\begin{pmatrix} S_u & \gamma_{uv} & \gamma_{uw} \\ & S_v & \gamma_{vw} \\ & & S_w \end{pmatrix}$$

FIG. 2. The Cartesian spectrum density matrix for the data shown in Fig. 1.

system is rotated. If topography is poorly known or navigation is poor, unnecessary errors will contaminate the description of the measurement.

3. The generalized spectrum density matrix

The description of a vector time series measurement given above has been in terms of a two-fold decomposition. The first was a frequency decomposition—the standard Fourier series representation. The second decomposition was in the representation of the Fourier component vector at a given frequency in terms of its components along three mutually orthogonal coordinate axes—a standard Cartesian representation. The Fourier component vector need not be described by its components along orthogonal axes, however, but can be represented by any basis set of motions which

span the three-dimensional space. Let the Fourier component vector be represented by

$$\hat{\mathbf{V}} = a_1\mathbf{e}_1 + a_2\mathbf{e}_2 + a_3\mathbf{e}_3. \tag{9}$$

The unit vectors $\mathbf{e}_i$ *each represent a particular type of motion.* For the Cartesian spectrum representation, the unit vectors are chosen to be

$$\mathbf{e}_1 = \begin{pmatrix} 1 \\ 0 \\ 0 \end{pmatrix}, \quad \mathbf{e}_2 = \begin{pmatrix} 0 \\ 1 \\ 0 \end{pmatrix}, \quad \mathbf{e}_3 = \begin{pmatrix} 0 \\ 0 \\ 1 \end{pmatrix}, \tag{10}$$

representing rectilinear motion along the x, y and z axes, respectively. The (complex) amplitudes a_i tell how much motion (and of what phase) of the type represented by $\mathbf{e}_i$ is present as a function of frequency. It may be thought of as a generalized Fourier coefficient. The amplitudes a_i are found by projection onto the corresponding unit vector, thus

$$a_i = \mathbf{e}_i^* \cdot \hat{\mathbf{V}}. \tag{11}$$

Generally the unit vectors are chosen to be orthonormal, $\mathbf{e}_i^* \cdot \mathbf{e}_j = \delta_{ij}$, to simplify the calculations and interpretations. In the case of the Cartesian representation, the generalized amplitudes reduce to the previous case, *viz.*, $a_i = \hat{u}_i$. A generalized spectrum density matrix can now be defined by

$$S_{ij} \equiv \langle a_i^* a_j \rangle \tag{12}$$

and generalized coherences are given by

$$\gamma_{ij} \equiv \frac{\langle a_i^* a_j \rangle}{[\langle a_i^* a_i \rangle \langle a_j^* a_j \rangle]^{1/2}}. \tag{13}$$

If a Cartesian spectral representation $\mathbf{S}^{(c)}$ has been computed, one need not start all over with different unit vectors to find the generalized Fourier coefficients and then the generalized SDM. Instead, it can be shown that any generalized SDM can be found from the Cartesian SDM, by using the appropriate (orthonormal) unit vectors to transform the spectrum

$$S_{ij} \equiv \langle a_i^* a_j \rangle \equiv \mathbf{e}_i^* \cdot \mathbf{S}^{(c)} \cdot \mathbf{e}_j, \tag{14}$$

thereby providing a saving in computer time. (The generalized Fourier amplitudes are still needed to compute coherences with components of a different vector time series, however.) For a multiple-vector time series, the cross-spectrum density matrix generalizes in the same way. If, for example, two Fourier component vectors are represented by

$$\hat{\mathbf{V}} = \sum_{i=1}^{3} a_i^{(1)}\mathbf{e}_i^{(1)} \quad \text{and} \quad \hat{\mathbf{U}} = \sum_{i=1}^{3} a_i^{(2)}\mathbf{e}_i^{(2)}, \tag{15}$$

where $\mathbf{e}_i^{(1)}$ and $\mathbf{e}_i^{(2)}$ are (possibly) different unit vectors, the elements of the generalized CSDM are given by

$$S_{ij}^{1,2} = \langle \hat{a}_i^{(1)*} \hat{a}_i^{(2)} \rangle \tag{16}$$

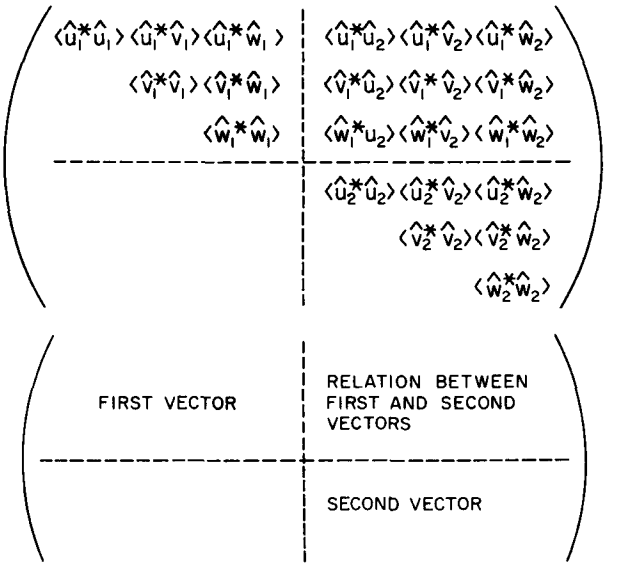

FIG. 3. The two-vector three dimensional cross-spectrum density matrix in the Cartesian representation.

with obvious extensions to more than two vectors. Most often, the unit vectors will be chosen to be the same, *viz.*, $\mathbf{e}_i^{(1)} = \mathbf{e}_i^{(2)}$.

4. Rotational invariants

Before proceeding with the development of generalized spectrum representations, it is useful to exploit some special properties of the Cartesian SDM.

The actual measurements made by a current meter are referred to a particular coordinate system. It is useful to find spectrum quantities which are independent of the orientation of the coordinate system. Such quantities would then be unaffected by errors in the coordinate orientation caused by compass and navigational errors, poorly defined topography, etc. Since the elements of the Cartesian SDM are defined in terms of vector components, this SDM is actually a tensor and automatically has properties which are independent of coordinate system rotation.

Simple versions of the invariants hold true for rotations in a plane, for example, those rotations about a fixed vertical axis. Fofonoff (1969) looked for these latter invariants by actually rotating the coordinate system and combining quantities appropriately. The usefulness of any spectrum invariant depends on how it can be related to quantities of physical interest. The spectrum invariants and their interpretations are as follows:

a. The trace

The trace of the Cartesian spectrum density tensor is the most easily computed and interpreted of the spectral invariants. The trace is

$$\mathrm{Tr}\mathbf{S} \equiv \sum_{i=1}^{3} S_{ii} = 2 \times \text{total kinetic energy}, \quad (17a)$$

$$\mathrm{Tr}_H\mathbf{S} \equiv \sum_{i=1}^{2} S_{ii} = 2 \times \text{horizontal kinetic energy}, \quad (17b)$$

where the identification with kinetic energy has been made on the basis of $S_u \equiv \langle \hat{u}_i^* \hat{u}_i \rangle = |\hat{u}_i|^2$ and kinetic energy $= \frac{1}{2}|\hat{u}_i|^2$.

b. The determinant

The determinant of the three-dimensional SDM can be written as

$$|\mathbf{S}| = S_{11}S_{22}S_{33}(1 - |\delta_{12}|^2 - |\delta_{23}|^2 - |\delta_{31}|^2 + 2\,\mathrm{Re}\Gamma), \quad (18a)$$

where $\Gamma \equiv \gamma_{12}\gamma_{23}\gamma_{31}$ and γ_{ij} are the complex coherences. In 2-D this reduces to

$$|\mathbf{S}|_H = S_{11}S_{22}(1 - |\gamma_{12}|^2). \quad (18b)$$

It can be seen that the determinant is in some sense a measure of incoherent noise. By analogy with the description of partially coherent light (Born and Wolf, 1970), a measure of the fraction of nonrandom and non-isotropic energy, called the degree of polarization P may be defined by

$$P^2 \equiv 1 - \frac{|\mathbf{S}|_H}{(\frac{1}{2}\,\mathrm{Tr}_H\mathbf{S})^2} \quad (19)$$

which is also exactly the same as Fofonoff's maximum coherence parameter. P is real and varies between zero and unity. A related parameter giving the ratio of nonrandom non-isotropic to random and isotropic energy (which may be thought of as a signal to noise ratio), is called the anisotropy ratio A, where

$$A \equiv \frac{P}{1 - P}. \quad (20)$$

The anisotropy ratio may be much greater than unity at a tidal frequency, for example.

c. The sum of principal minors

The sum of principal minors can be written as

$$M \equiv \sum_{i=1}^{3} M_{ii} = \tfrac{1}{2} \sum_{i \neq j} S_{ii}S_{jj}(1 - |\gamma_{ij}|^2). \quad (21)$$

Each principal minor is recognized as a 2-D determinant in one of the coordinate planes. An interpretation can be attached to M relating it to P defined above. A mean degree of polarization $\tilde{P}$ (and corresponding mean anisotropy ratio) in the coordinate planes may be defined

$$\tilde{P}^2 \equiv 1 - \frac{M}{(\mathrm{Tr}\mathbf{S})^2}, \quad (22)$$

which is still invariant, though perhaps not as useful as P itself.

d. The total squared quadrature spectrum

The last of this class of spectrum invariants is

$$Q^2 \equiv \tfrac{1}{2} \sum_{i \neq j} (S_{ij} - S_{ji})^2 \equiv \tfrac{1}{2} \sum_{i \neq j} Q_{ij}^2. \quad (23)$$

Suppose for the moment that a 2-D spectrum has been measured. It is shown in the next section that the quadrature spectrum describes the *net* amount of rotating energy in a plane. A "rotary coefficient" giving the fraction of net rotating energy is defined by

$$C_{r_H} \equiv \frac{Q_H}{\frac{1}{2}\,\mathrm{Tr}_H\mathbf{S}}, \quad (24a)$$

where the subscript H refers to, say, the horizontal plane. This rotary coefficient is invariant to rotations of the coordinate system in that plane. In general, there is a different rotary coefficient for each coordinate plane. For general rotations the mean rotary coefficient defined by

$$\bar{C}_r \equiv \frac{Q}{\frac{1}{2}\,\mathrm{Tr}\mathbf{S}} \quad (24b)$$

is invariant.

e. Multiple coherence

A measure of the total coherence between the vertical and *both* horizontal velocity components is the ordinary multiple coherence γ_{312} which can be written as

$$\gamma_{312} \equiv 1 - \frac{|\mathbf{S}|}{S_{33}M_{33}}, \quad (25)$$

where M_{33} is the third principal minor. Since S_{33} and M_{33} are invariant only for rotations about the vertical axis, the multiple coherence will only be invariant in that case. [The partial coherence and partial phase can easily be written in terms of the elements of the Cartesian SDM, however, they are not invariant under coordinate rotations. For further discussion of these parameters see for example, Jenkins and Watts, (1968).] Some of the spectrum invariants for the data of Fig. 1 are shown in Fig. 4. We return now to the discussion of the generalized spectrum density matrix.

5. Rotary spectra

a. The rotary representation

A common alternative to the Cartesian spectrum representation described above is the rotary representation. In this representation the Fourier vector is decomposed into two counterrotating circular motions in a plane, usually (though not

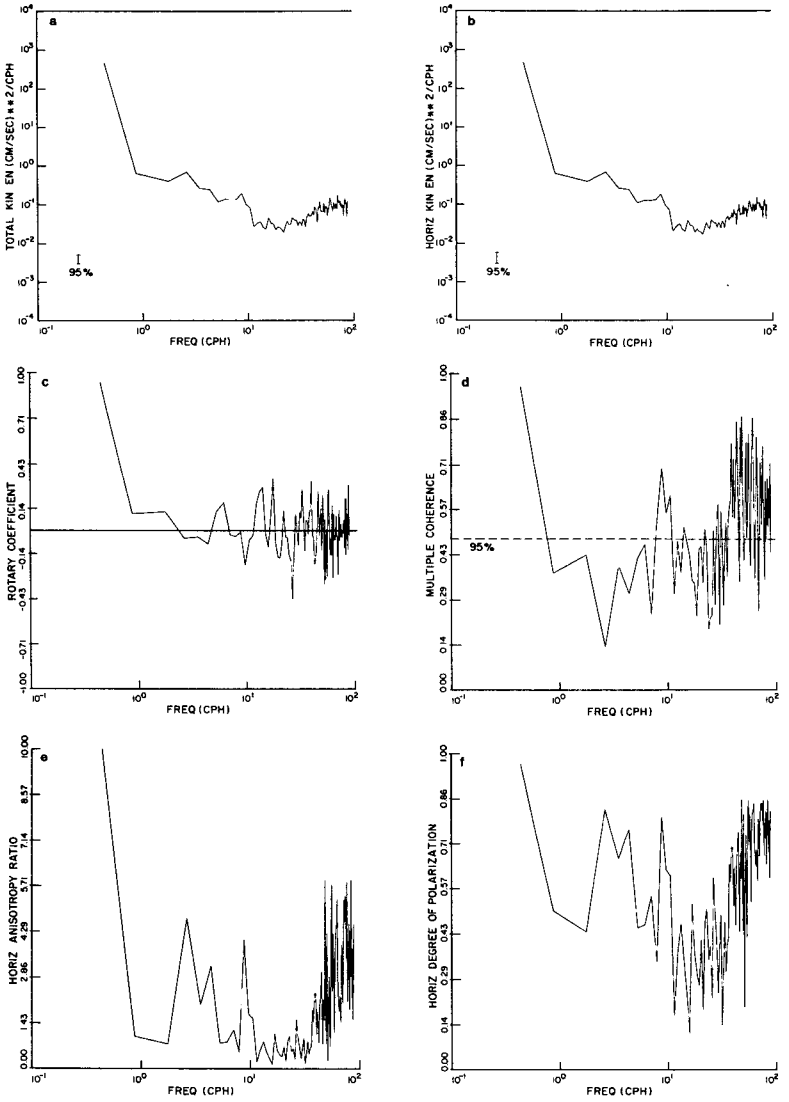

FIG. 4. Rotational invariants for the data shown in Fig. 1.

always the best choice) taken as the horizontal plane. In three dimensions a linear oscillation normal to the plane of the rotary vectors is added. Writing out the decomposition directly gives

$$\hat{\mathbf{V}}_m = \begin{pmatrix} u_1 e^{i\theta_1} \\ u_2 e^{i\theta_2} \\ u_3 e^{i\theta_3} \end{pmatrix} = C_1 \begin{pmatrix} u_1 e^{i\theta_1} \\ u_1 e^{i(\theta_1+\pi/2)} \\ 0 \end{pmatrix} + C_2 \begin{pmatrix} u_1 e^{i\theta_1} \\ u_1 e^{i(\theta_1-\pi/2)} \\ 0 \end{pmatrix} + C_3 \begin{pmatrix} 0 \\ 0 \\ u_3 e^{i\theta_3} \end{pmatrix} . \quad (26)$$

By the general formalism of the previous section this decomposition can be written as in Eq. (9), where the unit vectors $\mathbf{e}$ correspond to those on the right side of Eq. (26), *viz.*,

$$\mathbf{e}_1 = 2^{-1/2} \begin{pmatrix} 1 \\ i \\ 0 \end{pmatrix}, \quad \mathbf{e}_2 = 2^{-1/2} \begin{pmatrix} 1 \\ -i \\ 0 \end{pmatrix}, \quad \mathbf{e}_3 = \begin{pmatrix} 0 \\ 0 \\ 1 \end{pmatrix} \quad (27)$$

and represent counterclockwise and clockwise circular motion in the horizontal plane and vertical motion, respectively. Note that these unit vectors form a complete orthonormal set for the three-dimensional space. The generalized Fourier coefficients are found by projecting the unit vectors onto the original Cartesian Fourier component vector

$$a_1 = a_+ = \mathbf{e}_1^* \cdot \mathbf{V} = 2^{-1/2}(\hat{u}_1 - i\hat{u}_2), \quad (28a)$$

$$a_2 = a_- = \mathbf{e}_2^* \cdot \mathbf{V} = 2^{-1/2}(\hat{u}_1 + i\hat{u}_2), \quad (28b)$$

$$a_3 = \mathbf{e}_3^* \cdot \mathbf{V} = \hat{u}_3, \quad (28c)$$

where $\hat{u}_1 \equiv u_1 e^{i\theta_1}$, etc.

The elements of the generalized SDM can be found either from the rotary Fourier coefficients given above, using (12), or directly from the Cartesian SDM and the rotary unit vectors, using Eq. (14). The results are often conveniently written in terms of the spectrum invariants. In any case the rotary spectrum elements are found to be given by

$$S_{11} = S_+ = \langle a_1^* a_1 \rangle = \tfrac{1}{2}[\langle \hat{u}_1^* \hat{u}_1 \rangle + \langle \hat{u}_2^* \hat{u}_2 \rangle - 2Q_{12}] = \tfrac{1}{2}\,\mathrm{Tr}_H\mathbf{S}(1 - C_r), \quad (29a)$$

where $C_r = Q_{uv}/\mathrm{Tr}_H\mathbf{S}$ and all the elements in the last two expressions on the right are computed from the Cartesian SDM. Similarly,

$$S_{22} = S_- = \langle a_2^* a_2 \rangle = \tfrac{1}{2}\,\mathrm{Tr}_H\mathbf{S}(1 + C_r), \quad (29b)$$

$$S_{33} = \langle a_3^* a_3 \rangle = \langle \hat{u}_3^* \hat{u}_3 \rangle = S_w. \quad (29c)$$

Here $S_\pm$ are the rotary spectra (corresponding to the "inner autospectra" of Mooers). The interpretation of the rotary coefficient as the fraction of net rotating energy comes from the fact that it can be written as

$$C_r = \frac{S_+ - S_-}{S_+ + S_-} . \quad (30)$$

The normalized cross-spectrum element is the rotary coherence,

$$\gamma_{12} = \frac{S_{12}}{(S_{11}S_{22})^{1/2}} = \gamma_{+-} = \frac{\tfrac{1}{2}(S_{uu} - S_{vv}) - iC_{uv}}{\tfrac{1}{2}(\mathrm{Tr}_H\mathbf{S})(1 - C_r^2)^{1/2}} \equiv |\gamma_{+-}| e^{i\phi_{+-}} \quad (31a)$$

(where C_{uv} is the cospectrum of u and v, C_r is the rotary coefficient, etc., all from the Cartesian SDM). We find that

$$|\gamma_{+-}|^2 = (P^2 - C_r^2)/(1 - C_r^2), \quad (31b)$$

$$\tan\phi_{+-} = 2C_{uv}/(S_{vv} - S_{uu}). \quad (31c)$$

Gonella called $|\gamma_{+-}|$ the "stability" and related it to the vector hodograph (discussed below). Mooers called the cross-spectrum element $S_{12} \equiv S_{+-} \equiv \langle a_\pm^* a_- \rangle$ the "outer-autospectrum" and identified its relation to the coherence between counter-rotating wave components. In three dimensions the remaining spectrum elements describe the coherence between the vertical and each of the rotating components:

$$\gamma_{\pm w} = \frac{\langle a_\pm^* a_3 \rangle}{[\langle a_\pm^* a_\pm \rangle \langle a_3^* a_3 \rangle]^{1/2}} = \frac{1}{\sqrt{2}} \frac{(S_{uw} \pm iS_{vw})}{(S_\pm S_w)^{1/2}} \quad (32)$$

In principle these coherences can be related to the three-dimensional hodograph, but the hodograph is more simply described by other parameters which will be introduced. The rotary representation of the data of Fig. 1 is shown in Fig. 5.

Like the rotational invariants, the rotary representation shares in the advantage of being insensitive to errors in coordinate system orientation (for rotation in the plane of the rotary unit vectors). There are situations in which it is advantageous to take the rotary spectra in a different plane. For example, one expects internal waves propagating into shallower water will increase in amplitude until they overturn and break. Rotary unit vectors in a vertical plane aligned perpendicularly to the topography will be the most sensitive way of picking out that particular type of motion. These unit vectors can be obtained from the ones given above by an appropriate rotation of the coordinate system. Similarly, the rotary spectra can be made into elliptical spectra of any aspect ratio by changing the relative amplitude of the components if there is reason to want to identify motions of that type (surface waves over a flat bottom, for example).

b. Simple motions in the rotary representation

Before moving on to other spectral representations it is instructive to look at the same two simple

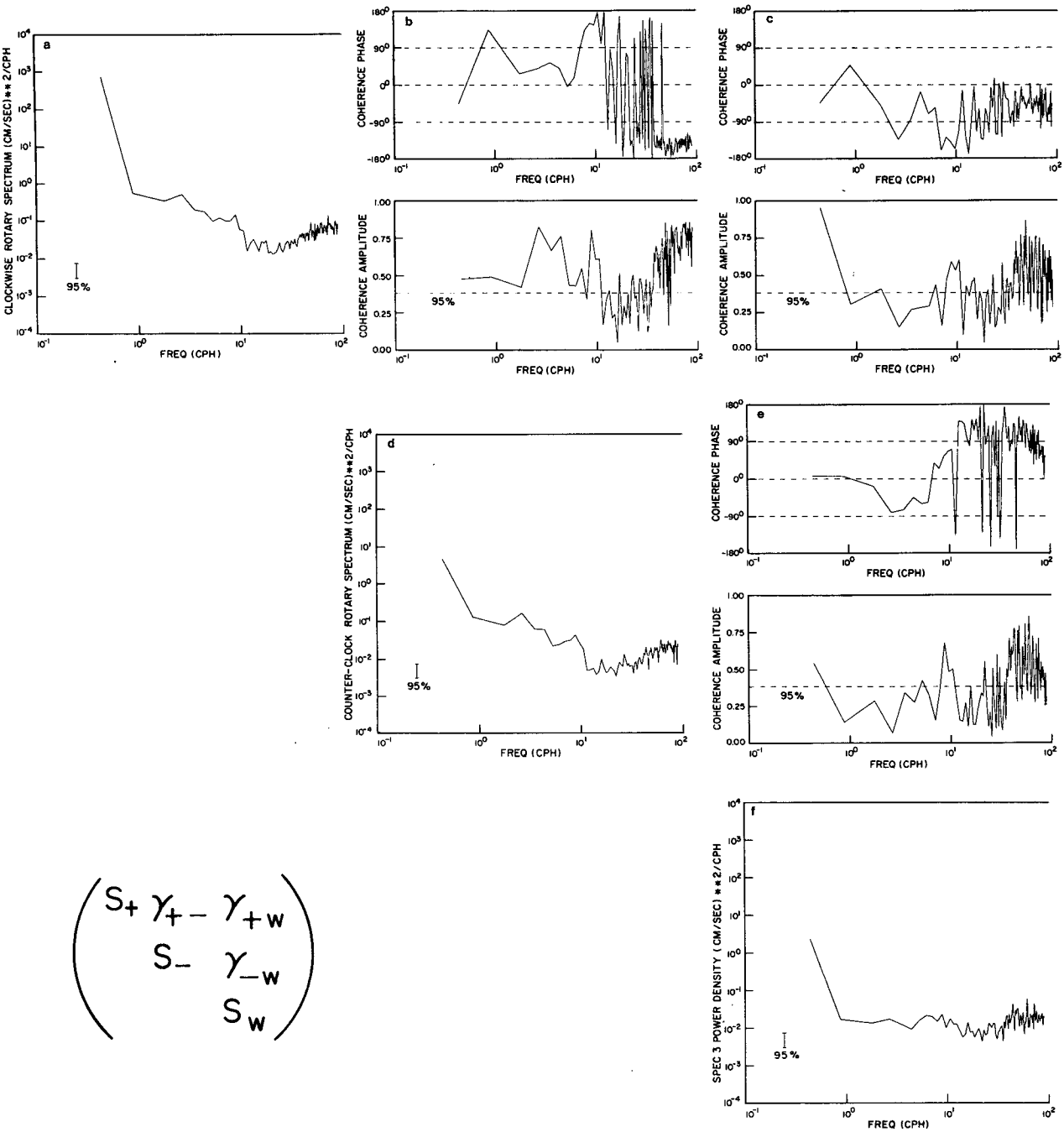

$$\begin{pmatrix} S_+ & \gamma_{+-} & \gamma_{+w} \\ & S_- & \gamma_{-w} \\ & & S_w \end{pmatrix}$$

FIG. 5. Rotary representation of the data shown in Fig. 1.

motions used to illustrate the Cartesian SDM, to see what the rotary representation looks like in these cases.

1) RECTILINEAR MOTION

If the motion is rectilinear along $\mathbf{r} = \alpha\mathbf{i} + \beta\mathbf{j} + \gamma\mathbf{k}$ with $\hat{\mathbf{V}} = a_0 e^{i\theta}(\alpha\beta\gamma)^{\mathrm{T}}$, the rotary Fourier amplitudes are found to be

$$a_+ = (a_0/\sqrt{2})(\alpha + i\beta), \quad a_- = (a_0/\sqrt{2})(\alpha - i\beta), \quad a_3 = a_0\gamma, \tag{33a}$$

which give matrix elements

$$S_{11} = S_+ = \tfrac{1}{2}a_0^2(\alpha^2 + \beta^2) = S_{22} = S_-, \quad S_{33} = S_w = a_0^2\gamma^2, \tag{33b}$$

$$S_{+-} = \tfrac{1}{2}a_0^2(\alpha^2 + \beta^2), \quad S_{\pm w} = \tfrac{1}{2}a_0^2\gamma(\alpha \pm i\beta). \tag{33c}$$

We see that the rotary representation for linear motion is inefficient in the sense that many spectral elements are nonzero and complex even for this simple motion. Compare the cartesian representation [Eq. (7)] for general linear motion given above.

2) CIRCULAR MOTION

Suppose the motion is clockwise and circular in the horizontal plane (as in the case for inertial motion, for example). The rotary SDM is then

$$\mathbf{S} = a_0^2 \begin{pmatrix} 0 & 0 & 0 \\ & 1 & 0 \\ & & 0 \end{pmatrix}, \tag{34}$$

where a_0 gives the strength of the motion. Compare the Cartesian representation (8) of this motion given above.

These two examples have hinted at the importance of using a good representation to pick out motions of interest. The appropriate representation can simplify the task of interpretation considerably. In more complicated or unknown motions different representations are more appropriate, and can be found *a posteriori* or specified *a priori*.

6. Empirical eigenmode spectra

a. Empirical kinematic normal modes

The Cartesian and rotary representations of the vector spectrum described above were chosen *a priori* and arbitrarily for ease of interpretation. In principle, any set of unit vectors (i.e., wave types) which span the space may be chosen as the basis set for the spectrum representation. A natural set to use is the orthonormal set of eigenvectors $\mathbf{g}_i$ of the Cartesian SDM, which are obtained from the eigenvalue equation

$$\mathbf{S}\mathbf{g}_i = \lambda_i \mathbf{g}_i. \tag{35}$$

These eigenvectors form a complete orthonormal set and can be thought of as the kinematic normal modes for the time series measurements. The eigenvectors change with frequency, so the type of motion each represents must be interpreted (by studying "behavior" of the vector hodograph, discussed below) for each frequency (unlike the Cartesian or rotary unit vectors which have the same amplitude and phase relations at all frequencies). As in the Cartesian and rotary representations [Eqs. (9), (10) and (27)] the Fourier component vector is now expanded in the eigenvectors

$$\hat{\mathbf{V}} = a_1\mathbf{g}_1 + a_2\mathbf{g}_2 + a_3\mathbf{g}_3. \tag{36a}$$

By using the orthonormal property of the eigenvectors, and the eigenvalue equation, it can be shown that the coefficients in Eq. (36a) are the eigenvalues. Thus

$$\hat{\mathbf{V}} = \lambda_1^{1/2}\mathbf{g}_1 + \lambda_2^{1/2}\mathbf{g}_2 + \lambda_3^{1/2}\mathbf{g}_3, \tag{36b}$$

a result known as Mercer's theorem. Since the SDM is Hermitian, all the eigenvalues are real. In the empirical eigenmode representation spectrum amplitudes are given by the diagonal elements, $S_{ii} = \lambda_i$. The coherences between modes are obtained from Eq. (14), but in the case of an empirical eigenmode representation there is an important simplification. Suppose $\mathbf{e}_i = \mathbf{g}_i$ and we use the eigenvalue equation (35) in Eq. (14). Then $\langle a_i^* a_j \rangle = \mathbf{g}_i^* \cdot \mathbf{S}^{(c)} \cdot \mathbf{g}_j = \lambda_j \delta_{ij}$, and it follows that all the coherences between eigenvectors are zero. The three modes are independent and therefore only the three real diagonal elements of the SDM are nonzero. The empirical mode spectra for the data of Fig. 1 are shown in Fig. 6. This is indeed a simple characterization of a vector spectrum. This simplification is at the expense of a more complicated hodograph associated with each eigenvector, both of which are now functions of frequency. The eigenvector hodographs will be discussed in the next section. These eigenvector hodographs which would be similar in appearance to those of Fig. 7 are not shown. It is important to recognize that these empirical modes are not a property of any geometry (as in the case of normal modes of a basin) nor do they depend on any dynamical assumptions (as in the case of "empirical modes" for vertical structure when stratification varies) but rather they are a property of the time series itself. Wallace and Dickenson (1972) also discuss this type of spectral representation.

b. Simple examples of empirical modes

1) LINEAR MOTION

Suppose, as in the previous examples, the motion is linear along an arbitrary direction given by $\Gamma = \alpha\mathbf{i} + \beta\mathbf{j} + \gamma\mathbf{k}$. Then the Cartesian SDM is

$$\mathbf{S} = \langle a_0^2 \rangle \begin{pmatrix} \alpha^2 & \alpha\beta & \alpha\gamma \\ & \beta^2 & \beta\gamma \\ & & \gamma^2 \end{pmatrix}, \tag{37}$$

where a_0 is the amplitude of the motion. What are the empirical modes? The secular equation resulting from Eq. (37) leads to eigenvalues

$$\lambda_1 = \langle a_0^2 \rangle (\alpha^2 + \beta^2 + \gamma^2), \quad \lambda_2 = \lambda_3 = 0. \tag{38}$$

The unit magnitude eigenvector for λ_1 turns out to be

$$\mathbf{g}_1 = N_1 \begin{pmatrix} \alpha \\ \beta \\ \gamma \end{pmatrix}, \tag{39}$$

where $N_1 \equiv (\alpha^2 + \beta^2 + \gamma^2)^{-1/2}$ and it represents linear motion along $\mathbf{r}$. The other two eigenvalues are degenerate, so their eigenvectors are inde-

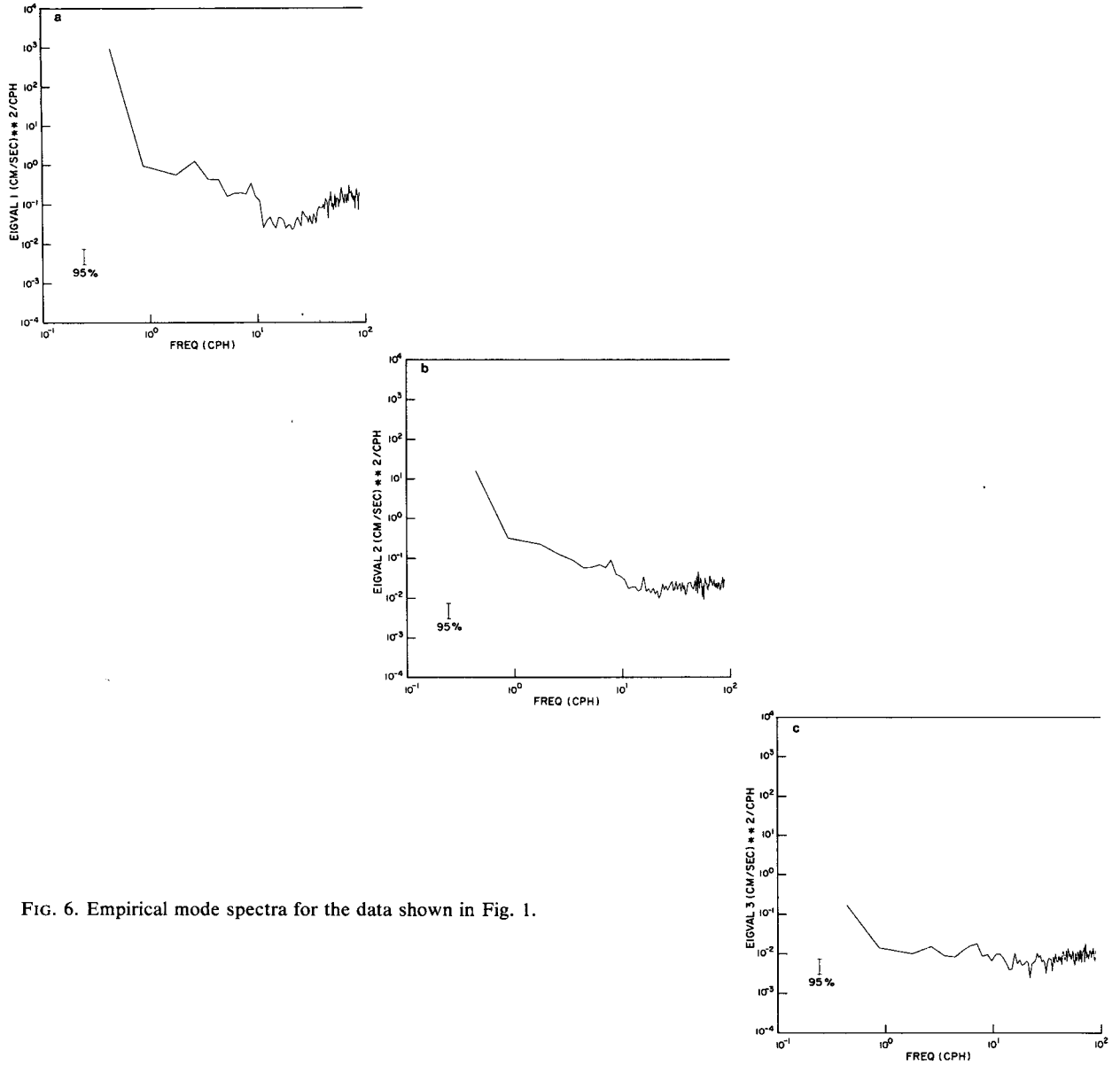

FIG. 6. Empirical mode spectra for the data shown in Fig. 1.

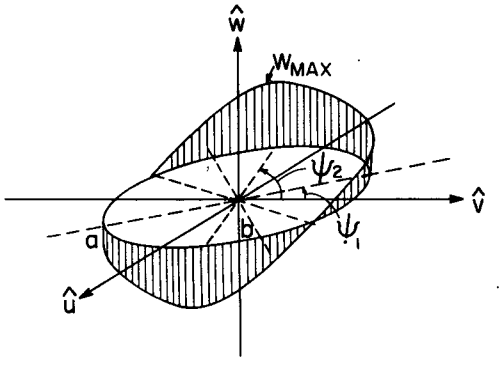

FIG. 7. The three-dimensional Fourier vector hodograph. The five parameters which specify the shape of the hodograph are indicated.

terminate. These two eigenvectors must satisfy the eigenvalue equation, which leads to

$$\frac{z_i}{x_i} = -\frac{\beta}{\gamma}\frac{y_i}{x_i} - \frac{\alpha}{\gamma},$$

where

$$\mathbf{g}_i = \begin{pmatrix} x_i \\ y_i \\ z_i \end{pmatrix}, \quad i = 2, 3, \tag{40}$$

which implies, by Eq. (39), that $\mathbf{g}_1^* \cdot \mathbf{g}_2 = 0$ and $\mathbf{g}_1^* \cdot \mathbf{g}_3 = 0$.

The other two eigenvectors represent motion in a plane perpendicular to $\mathbf{r}$. They may be chosen so that $\mathbf{g}_2 \cdot \mathbf{g}_3 = 0$ as well. All of the energy is contained in the first eigenmode.

2) ELLIPTIC MOTION

Suppose, as in the case of plane surface waves over a flat bottom, the particle motion is elliptical in a vertical plane. Suppose also, for generality, that this vertical plane makes an angle ψ with the $\hat{u}$ axis. The Fourier component velocity vector is then

$$\hat{\mathbf{V}} = \begin{pmatrix} u_0 \cos\psi e^{i\theta} \\ u_0 \sin\psi e^{i\theta} \\ w_0 e^{i(\theta \pm \pi/2)} \end{pmatrix}, \tag{41}$$

where the $\pm$ sign in w indicates the two senses of rotation. (If $\psi = 0$, $u_0 = w_0$ and the $-$ sign is chosen in w, then the motion is circular in the w–z plane and is clockwise looking toward the origin from $+v$). The Cartesian SDM resulting from the above measurement is [by Eq. (2)]

$$\mathbf{S} = \begin{pmatrix} \langle u_0^2 \cos^2\psi \rangle & \langle u_0^2 \cos\psi \sin\psi \rangle & \mp i\langle u_0 w_0 \cos\psi \rangle \\ & \langle u_0^2 \sin^2\psi \rangle & \mp i\langle u_0 w_0 \sin\psi \rangle \\ & & \langle w_0^2 \rangle \end{pmatrix}. \tag{42}$$

The eigenvalues in this case turn out to be

$$\lambda_1 = (u_0^2 + w_0^2), \quad \lambda_2 = 0, \quad \lambda_3 = 0. \tag{43}$$

The first unit eigenvector is found to be by the secular Eq. (35)

$$\mathbf{g}_1 = N_1 \begin{pmatrix} u_0 \cos\psi \\ u_0 \sin\psi \\ \pm i w_0 \end{pmatrix}, \quad \text{where} \quad N_1 \equiv \lambda_1^{-1/2}. \tag{44}$$

The other two eigenvectors must satisfy (by the secular equation)

$$\frac{y_i}{x_i} = \frac{\pm i w_0}{u_0 \sin\psi}\frac{z_i}{x_i} - \frac{\cos\psi}{\sin\psi},$$

where

$$\mathbf{g}_i = \begin{pmatrix} x_i \\ y_i \\ z_i \end{pmatrix}, \quad i = 2, 3. \tag{45}$$

They may be chosen so that the three form an orthonormal triad:

$$\mathbf{g}_1^* \cdot \mathbf{g}_2 = 0, \quad \mathbf{g}_1^* \cdot \mathbf{g}_3 = 0, \quad \mathbf{g}_2^* \cdot \mathbf{g}_3 = 0, \tag{46}$$

which, because of the degeneracy, is not unique. For example choosing $y_2/x_2 = \tan\psi$, the second unit vector is

$$\mathbf{g}_2 = N_2 \begin{pmatrix} u_0 \cos\psi \\ u_0 \sin\psi \\ \mp i(u_0^2/w_0) \end{pmatrix},$$

$$N_2 \equiv [u_0^2(1 + u_0^2/w_0^2)]^{-1/2} \tag{47}$$

which is the oppositely rotating wave in the same plane as $\mathbf{g}_1$. When $u_0 = v_0$ these two unit vectors are the rotary spectra in the plane of rotation. The third unit vector, chosen to be orthogonal to the first two and to satisfy (45) is

$$\mathbf{g}_3 = N_3 \begin{pmatrix} 1 \\ -\cot\psi \\ 0 \end{pmatrix}, \quad N_3 \equiv [u_0^2(1 + \cot^2\psi)]^{-1/2} \tag{48}$$

which represents horizontal rectilinear motion along the normal to the plane in which the rotation is occurring.

These two examples illustrate the nature of the eigenvector representation in simple cases. In general, the motion does not occur in a plane, there is neither degeneracy nor eigenvalues equal to zero, and all empirical modes are important. The general case is discussed after the next section, in which hodographs are introduced.

7. Hodograph spectra

a. The vector hodograph

The hodograph is the curve traced out by the velocity vector as time progresses. Each Fourier component velocity vector, which in Cartesian form can be written as

$$\hat{\mathbf{V}}_m = \begin{pmatrix} u_0 e^{i(f_m t + \theta_1)} \\ v_0 e^{i(f_m t + \theta_2)} \\ w_0 e^{i(f_m t + \theta_3)} \end{pmatrix} = \begin{pmatrix} \hat{u}_1 \\ \hat{u}_2 \\ \hat{u}_3 \end{pmatrix}, \tag{49}$$

traces out its own hodograph with frequency f_m. For a given set of data, u_i and θ_i are fixed (they are coefficients in the Fourier expansion of the time series), so that the second of the above equations is a parametric representation of the hodograph, with t as parameter, for a given frequency. In general, the hodograph is a closed, three-dimensional curve. A common use of the two-dimensional hodograph, for example, is to characterize the tides by the size, shape, orientation and variability of the tidal ellipse. The properties of the hodograph depend only on how the water is moving around, not on the particular representation used to describe the spectrum. In other words, whether the motion is represented by Cartesian, rotary, empirical mode or other spectra, the parameters specifying the properties of

the hodograph must be equivalent. For convenience, the description of the hodograph will be given in terms of the Cartesian spectrum representation and the rotational invariants.

b. The two-dimensional hodograph

Since the two-dimensional hodograph (the ordinary current ellipse) is simpler and more familiar than its three-dimensional counterpart it will be investigated first. Eliminating t between the first two components of Eq. (49), gives

$$\left(\frac{\hat{u}_1}{u_0}\right)^2 + \left(\frac{\hat{u}_2}{v_0}\right)^2 - \frac{2\cos\delta}{u_0 v_0}\hat{u}_1\hat{u}_2 - \sin^2\delta = 0, \quad (50)$$

where $\delta \equiv \theta_1 - \theta_2$. This is the equation of a rotated ellipse in the $\hat{u}$, $\hat{v}$ coordinate plane. This equation is more conveniently manipulated in its matrix form, *viz.*,

$$\mathbf{Z}^{\mathrm{T}}\cdot\mathbf{H}\cdot\mathbf{z} = 1, \quad (51a)$$

where

$$\mathbf{z}^{\mathrm{T}} \equiv (\hat{u}\hat{v}) \quad \text{and} \quad \mathbf{H} \equiv \beta_0\begin{pmatrix}\beta_1 & -\beta_2\\ -\beta_2 & \beta_3\end{pmatrix}, \quad (51b)$$

$$\beta_0 \equiv \frac{1}{\sin^2\delta}, \quad \beta_1 \equiv \frac{1}{u_0^2},$$

$$\beta_2 \equiv \frac{\cos\delta}{u_0 v_0}, \quad \beta_3 \equiv \frac{1}{v_0^2}. \quad (51c)$$

Now in a coordinate system (denoted by a prime) aligned along the major and minor axes of the ellipse, the equation of the ellipse would be

$$\left(\frac{\hat{u}^1}{a}\right)^2 + \left(\frac{\hat{v}'}{b}\right)^2 = 1, \quad (52)$$

where a and b are the semi-major and semi-minor axes of the ellipse. In matrix form this equation can be written as

$$\mathbf{z}'^{\mathrm{T}}\cdot\mathbf{H}'\cdot\mathbf{z}' = 1, \quad (53)$$

where

$$\mathbf{z}'^{\mathrm{T}} \equiv (\hat{u}'\hat{v}') \quad \text{and} \quad \mathbf{H}' \equiv \begin{pmatrix}1/a^2 & 0\\ 0 & 1/b^2\end{pmatrix}.$$

A comparison of $\mathbf{H}$ and $\mathbf{H}'$ shows that if $\mathbf{H}$ is rotated into diagonal form, the diagonal elements will be reciprocals of the squares of the semi-major and semi-minor axes. This rotation can be performed in a standard way by using the unitary matrix T which is composed of the eigenvectors of $\mathbf{H}$, *viz.*, $\mathbf{T} \equiv (\mathbf{g}_1^H\mathbf{g}_2^H)$ where $\mathbf{H}\mathbf{g}_i^H = \lambda_i^H\mathbf{g}_i^H$. Then

$$\mathbf{T}^{\mathrm{T}}\cdot\mathbf{H}\cdot\mathbf{T} = \begin{pmatrix}\lambda_1^H & 0\\ 0 & \lambda_2^H\end{pmatrix} = \mathbf{H}' \quad (54)$$

so that $\lambda_1^H = 1/a^2$ and $\lambda_2^H = 1/b^2$. If λ_1^H is the smaller eigenvalue, the orientation of the major axis is given by the angle ψ,

$$\tan\psi = y/x \quad (55)$$

where the associated eigenvector is $\mathbf{g}_1^r = (xy)$. All that remains is to express the eigenvalue and eigenvectors of $\mathbf{H}$ in terms of the elements S_{ij} of the spectral density matrix, since it is these latter elements which are computed from the data. Comparing $\mathbf{S}$ to $\mathbf{H}$, and neglecting for the moment the effect of averaging, i.e., $\langle\ \rangle$ in $\mathbf{S}$, it turns out that

$$a^2 = \tfrac{1}{2}\,\mathrm{Tr}\mathbf{S}[1 + (1 - C_r^2)^{1/2}]$$
and
$$b^2 = \tfrac{1}{2}\,\mathrm{Tr}\mathbf{S}[1 - (1 - C_r^2)^{1/2}] \quad (56)$$

for the major and minor axes. Other useful parameters to describe the ellipse are

$$a^2 + b^2 = \mathrm{Tr}\mathbf{S} = 2 \times \text{kinetic energy}, \quad (57a)$$

$$ab = |Q| = 1/\pi \times \text{area of ellipse}, \quad (57b)$$

$$\epsilon = (1 - b^2/a^2)^{1/2} = \left[\frac{2(1 - C_r^2)^{1/2}}{1 + (1 - C_r^2)^{1/2}}\right]^{1/2} = \text{eccentricity}, \quad (57c)$$

$$b/a = \frac{1 - (1 - C_r^2)^{1/2}}{1 + (1 - C_r^2)^{1/2}} = \text{aspect ratio}. \quad (57d)$$

The principle axes of the ellipse are found from the eigenvectors and eigenvalues of H which are

$$\mathbf{g}_{1,2}^H = N_{1,2}\begin{pmatrix}1\\ \dfrac{\beta_0\beta_1 - \lambda_{1,2}^H}{\beta_0\beta_2}\end{pmatrix},$$

$$\lambda_{1,2}^H = \frac{1}{C_r^2\,\frac{1}{2}\mathrm{Tr}\mathbf{S}}[1 \pm (1 - C_r^2)^{1/2}] \quad (58)$$

where $N_{1,2}$ are normalization factors. The direction of the major axis is found by substituting for β_i and λ_i, the equivalent terms of the SDM, giving

$$\tan\psi_1 = (S_{22} - Q^2/a^2)/C. \quad (59)$$

An alternative form for ψ_1 can be found from the above expression by using the trigonometric identity $\tan 2\theta = 2\tan\theta/(1 - \tan^2\theta)$ and the secular equation for $\lambda = 1/a^2$ to eliminate the eigenvalue from the equation for ψ_1 to get the well-known expression (Fofonoff, 1969),

$$\tan 2\psi_1 = 2C/(S_{11} - S_{22}). \quad (60)$$

The angle ψ_1 is also equal to the phase of the generalized complex coherence in the rotary representation (Gonella, 1972).

In relating the matrix $\mathbf{H}$ to the SDM, the effect of averaging was neglected. In addition to the three parameters specifying the size, shape, and orientation of the two-dimensional hodograph ellipse, the statistical variability of the hodograph must also be specified. This description can be accomplished in several ways. Gonella and Mooers took the mag-

nitude of the rotary coherence $|\gamma_{+-}|$ as the statistical measure of variability of the major axis. The degree of polarization P or anisotropy ratio A also describe the variability. In principle the probability distributions of all the hodograph parameters (indeed all spectrum parameters) can be worked out (or at least approximated) and error bars put on all parameters. This distribution theory of spectrum estimates is discussed in another section.

Before proceeding to the three-dimensional hodograph, it is noted that a hodograph ellipse can be described by the Stokes parameters used to describe polarized light (Born and Wolf, 1970). These parameters are

$$\left.\begin{aligned} \alpha_0 &\equiv S_{11} + S_{22}, \quad \alpha_2 \equiv S_{12} + S_{21} = 2C \\ \alpha_1 &\equiv S_{11} - S_{22}, \quad \alpha_3 \equiv i(S_{21} - S_{12}) = -2Q \end{aligned}\right\}. \tag{61}$$

The ellipse size is then given by

$$\alpha_0 = a^2 + b^2. \tag{62a}$$

The shape is given by

$$b/a = \tan\chi \tag{62b}$$

where

$$\sin 2\chi = \frac{\alpha_3}{(\alpha_1^2 + \alpha_2^2 + \alpha_3^2)^{1/2}}$$

The orientation is

$$\tan 2\psi = \alpha_2/\alpha_1. \tag{62c}$$

For incoherent, isotropic motion, $\alpha_1 = \alpha_2 = \alpha_3 = 0$ so $\alpha_0^2 \geq \alpha_1^2 + \alpha_2^2 + \alpha_3^2$ which can be related to the degree of polarization by

$$P = (\alpha_1^2 + \alpha_2^2 + \alpha_3^2)^{1/2}/\alpha_0 \leq 1. \tag{62d}$$

c. *Three-dimensional and empirical mode hodographs*

Fortunately, the three-dimensional hodograph is a simple generalization of the two-dimensional one. Although it may have been expected that in three-dimensions the ellipse becomes an ellipsoid, this is not the case. In fact, as discussed above, in three-dimensions the hodograph remains a simple closed curve. This curve is wrapped around an elliptic cylinder, and it has the general appearance shown in Fig. 7. The two dimensional hodograph discussed above can be drawn in any coordinate plane, which has been taken as the horizontal in Fig. 7. Two additional parameters are needed to characterize the shape of the three-dimensional hodograph. If the 3-D Fourier vector is that of Eq. (49), the maximum departure from the horizontal plane is

$$w_{\max} = w_0 = S_w^{1/2}. \tag{63}$$

The second parameter describes the position of the vertical maximum on the horizontal ellipse (see Fig. 7). From (49), $\hat{w}$ is maximum when $f_m t = -\theta_3$. Letting primes denote $\hat{u}$ and $\hat{v}$ at the position of maximum $\hat{w}$, and substituting $f_m t = -\theta_3$ gives for ψ_2 (see Fig. 7),

$$\tan\psi_2 = \frac{\mathrm{Re}\hat{v}'}{\mathrm{Re}\hat{u}'} = \frac{\mathrm{Re}w_0\hat{v}'}{\mathrm{Re}w_0\hat{u}'} = \frac{\mathrm{Re}w_0 v_0 e^{i(\theta_2-\theta_3)}}{\mathrm{Re}w_0 u_0 e^{i(\theta_1-\theta_3)}} = \frac{\mathrm{Re}\hat{w}^*\hat{v}}{\mathrm{Re}\hat{w}^*\hat{u}} = \frac{C_{vw}}{C_{uw}}, \tag{64}$$

where C_{ij} are the cospectra. The hodograph representation for the data of Fig. 1 is shown in Fig. 8.

Hodograph analysis is essential for understanding empirical mode spectra. It was shown above that the eigenvalues of the Cartesian SDM give the power in the three independent empirical modes as a function of frequency (see Fig. 6). The empirical modes correspond to the eigenvectors of the Cartesian SDM. But what types of motion do the eigenvectors represent? Unlike the Cartesian or rotary unit vectors, the eigenvectors change with frequency; at each frequency, the type of motion they represent changes. To find out what this motion is, the hodograph, as a function of frequency, must be constructed for each eigenvector separately. The general procedure is as follows: first construct the Cartesian SDM and find its eigenvalues and eigenvectors, i.e., from $\hat{V} = (\hat{u}_1\hat{u}_2\hat{u}_3)'$ construct the Cartesian SDM, $S_{ij}^{(c)} = \langle \hat{u}_i^*\hat{u}_j \rangle$. Find the eigenvalues and eigenvectors

$$\mathbf{S}^{(c)}\mathbf{g}_k = \lambda_k \mathbf{g}_k, \tag{65}$$

where λ_k are eigenvalues and $\mathbf{g}_k = (\hat{x}_1\hat{x}_2\hat{x}_3)'$ are the eigenvectors. For each eigenvector construct the Cartesian SDM, $\tilde{\mathbf{S}}^{(c)}$

$$\tilde{S}_{ij}^{(c)} \equiv \langle \hat{x}_i^*\hat{x}_j \rangle \cdot \tag{66}$$

The hodograph of the eigenvector is now found from $\tilde{\mathbf{S}}^{(c)}$ by the method described above. In short, the eigenvector can be thought of as a Fourier component vector whose hodograph is to be found.

8. Prespecified spectra

In all of the previous spectral representations, the type of spectrum is either fixed and given (as in the Cartesian or rotary descriptions, where the motion is always linear or circular) or else the spectra change with frequency (as in the hodograph or empirical mode descriptions). This idea of a changing spectrum can be exploited to ease the task of interpreting the spectra. In all the cases just mentioned, the spectrum obtained from the measurements must be interpreted kinematically and dynamically. It is possible, in a sense, to reverse this procedure by using unit vectors of prespecified functional form. Thus instead of saying, "These are the measured spectra (of a certain type), now what do they mean?" one can say, "I am looking for

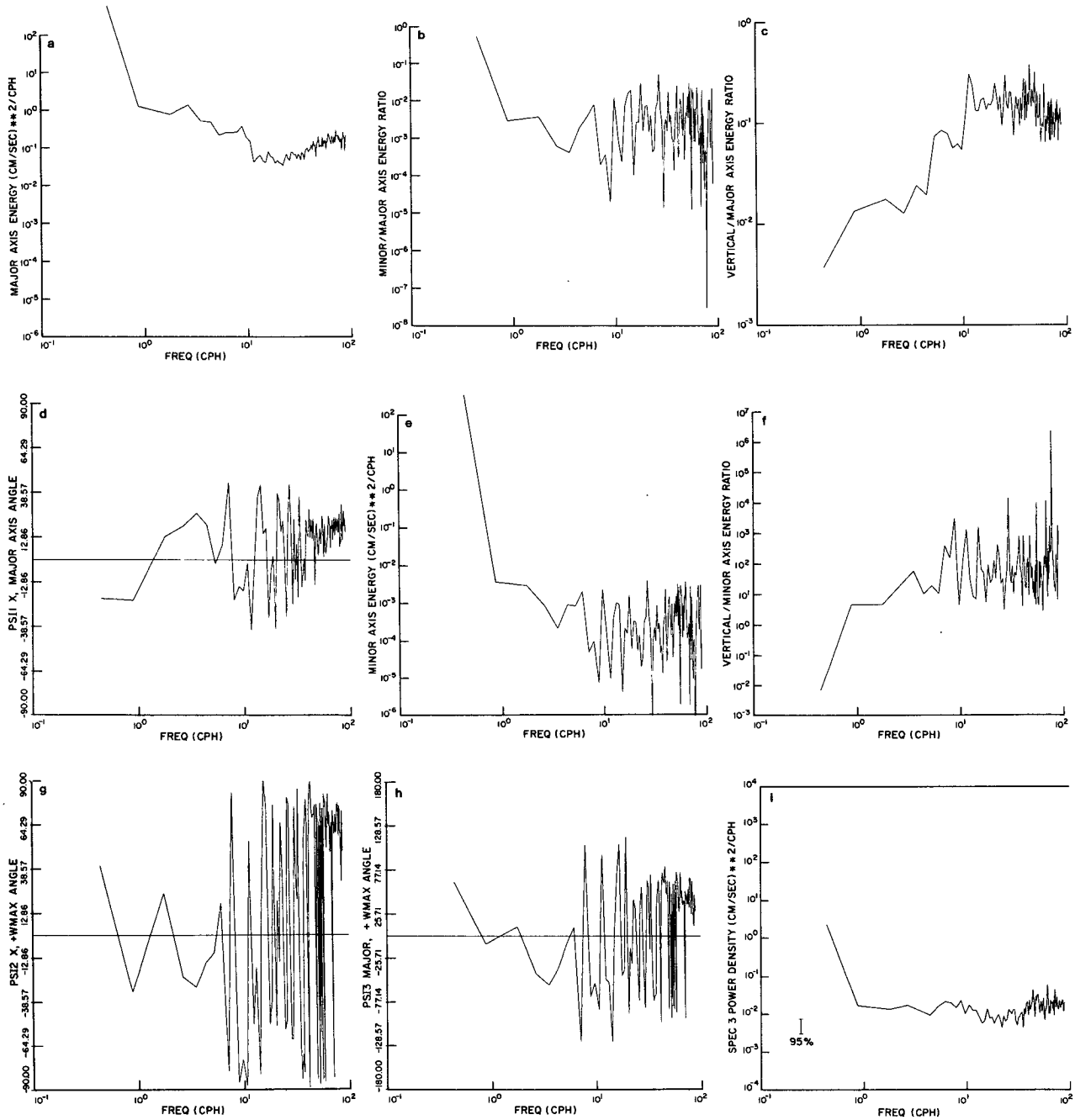

FIG. 8. Hodograph representation for the data shown in Fig. 1.

motion of a certain type (consistent with certain kinematic or dynamic assumptions); how much of the measured spectrum can be interpreted this way?" The unit vector $\mathbf{e}_1 = [\hat{u}(f)\hat{v}(f)\hat{w}(f)]'$ is constructed from theoretical arguments, two orthogonal unit vectors are found and the generalized spectrum density matrix is computed. The diagonal spectral element corresponding to $\mathbf{e}_1$ tells how much energy can be interpreted that way. This approach will become clearer in Part 2 of this paper, in which the general problem of dynamical testing is addressed.

9. Discussion of statistical errors

Any measurement is incomplete without a specification or at least a discussion of its accuracy. Error bars can be put on spectrum estimates once

their probability distributions are known. The question of the convergence of the sample spectrum to the "real" spectrum of the stochastic process has been of central importance in time series analysis (see, e.g., Jenkins and Watts, 1968). It is well-known that if the original data are normally distributed, the Fourier coefficients are normally distributed also. The smoothed sample spectral estimates (i.e., the diagonal elements of the Cartesian SDM) do converge and are then distributed as χ_ν^2, a chi-squared variable with ν degrees of freedom (associated with the smoothing). Error bars can then be put on these spectral estimates.

The distributions of the coherence amplitude and phase are more complicated than χ_ν^2. Nevertheless their distributions have been worked out (Amos and Koopmans, 1963) and error bars can be found. In the parameter range $\nu > 20$, $0.4 < \gamma < 0.95$ the error bars on coherence amplitude can be approximated by (Koopmans, 1974, p. 283)

$$\gamma_1 < \gamma < \gamma_2$$

$$\gamma_{1,2} = \tanh\left[\tanh^{-1}\hat{\gamma} \pm \frac{u_{\alpha/2}}{(2(\nu-1))^{1/2}} - \frac{1}{2(\nu-1)}\right], \quad (67)$$

where $u_{\alpha/2}$ is the $\alpha/2$ percentage point of the normal distribution and $\hat{\gamma}$ is the calculated coherence amplitude. In addition a level of zero significance, i.e., the coherence amplitude γ_0 below which the estimate is statistically indistinguishable from zero is given by (Koopmans 1974, p. 284, Jenkins and Watts 1968, p. 433).

$$\gamma_0 = \left[1 + \frac{(\nu-1)}{F_{2,2(\nu-1)}}\right]^{-1/2} \quad (68)$$

where $F_{\nu,\mu}$ is the F distribution. Tests to distinguish values of coherence other than zero can also be made (these are the "power tests" of Amos and Koopmans, 1963).

The error bars on coherence phase are (Koopmans, 1974, p. 285)

$$\hat{\theta} - \delta \le \theta \le \hat{\theta} + \delta, \quad (69)$$

where

$$\delta = \sin^{-1}\left\{\left[\frac{1-\hat{\gamma}^2}{\hat{\gamma}^2 2(\nu-1)}\right]^{1/2} t_{2(\nu-1)}^{(\alpha/2)}\right\},$$

where $t_\nu^{\alpha/2}$ is the $\alpha/2$ percentage point of the t-distribution with ν degrees of freedom.

It can be shown that the rotary representation spectrum parameters are distributed exactly as these Cartesian parameters, so all the results just summarized can be applied directly. Error bars in the other representations are more difficult to compute. Preliminary investigations show that the trace of the SDM may be approximated by χ^2, the rotary coefficient related to t, and the angle ψ_2 of the three-dimensional hodograph related to F distributions. The other parameters may be characterized by their lowest two moments—their biases and variances. However, more work is needed in this area before standard results may be applied.

10. Summary

The concept of a unit spectrum vector representing a particular type of motion has been used to relate and extend several approaches to the description of vector spectra. Each representation emphasizes different aspects of the flow and therefore has its advantages and disadvantages in various applications. The Cartesian representation best describes rectilinear motion and may be useful in describing the flow near strong topographic variations, for example. The rotary representation, rotational invariants and the shape of the hodograph are unaffected by errors in coordinate system definition. Using unit vectors, the rotary spectra can easily be taken in any plane. The empirical modes find independent orthogonal motions at the same frequency. They may be useful in separating motions at the same frequency which are due to different mechanisms or different waves, for example. By specifying a unit vector as a function of frequency, and constructing two other vectors orthogonal to it, the amount of energy consistent with certain hypotheses is automatically picked out. If the spectrum corresponding to the given unit vector contains more energy than the spectra of the other unit vectors, the motion has been largely "explained" by the dynamics that went into constructing the unit vector.

Any of the representations may be used for testing any proposed dynamical balance from a given measurement. The "best" representation depends both on the proposed dynamics and on other physical effects which may be present in the measurement. Several examples of dynamical testing in the different representations are given in Part 2.

Acknowledgments. I would like to thank Prof. Carl Wunsch for his encouragement, and Ms. Charmaine King for help with programming. This work was supported by ONR Contract N00014-75-C-0291.

REFERENCES

Amos, D. E., and Koopmans, L. H., 1963: Tables of the distribution of the coefficient of coherence for stationary bivariate Gaussian processes. *Monogr. SCR-483*, Sandia Corp., Albuquerque.

Born, M., and Wolf, E., 1970: *Principles of Optics*, 4th ed. Pergamon Press, 808 pp.

Calman, J., 1978: On the interpretation of ocean current spectra, Part 2: testing dynamical hypotheses. *J. Phys. Oceanogr.*, **8,** 644–652.

Fofonoff, N. P., 1969: Spectral characteristics of internal waves in the ocean. *Deep-Sea Res.* **16**(Suppl.), 59–71.

Gonella, J., 1972: A rotary-component method for analyzing meteorological and oceanographic vector time series. *Deep-Sea Res.*, **19,** 833–846.

Jenkins, G. M., and Watts, D. G., 1968: *Spectral Analysis and its Applications*. Holden-Day, 525 pp.

Koopmans, L. H., 1974: *The Spectral Analysis of Time Series*. Academic Press, 366 pp.

Mooers, C. N. K., 1973: A technique for the cross-spectrum analysis of pairs of complex-valued time series, with emphasis on properties of polarized components and rotational invariants. *Deep-Sea Res.*, **23,** 613–628.

Pollard, R. T., and R. C. Millard, Jr., 1970: Comparison between observed and simulated wind-generated inertial oscillations. *Deep-Sea Res.*, **17,** 813–821.

Thompson, R., and J. R. Luyten, 1976: Evidence for bottom-trapped topographic Rossby waves from single moorings. *Deep-Sea Res.*, **23,** 629–635.

Wallace, J. M., and Dickenson, R. E., 1972: Empirical orthogonal representation of time series in the frequency domain, Part 1: Theoretical considerations. *J. Appl. Meteor.*, **11,** 887–892.